



HAL
open science

A innovative modeling approach to investigate the efficiency of cross flow water turbine farms

Sylvain Antheaume, Thierry Maître, Jean-Luc Achard

► **To cite this version:**

Sylvain Antheaume, Thierry Maître, Jean-Luc Achard. A innovative modeling approach to investigate the efficiency of cross flow water turbine farms. 2nd IAHR International Meeting of the Workgroup on Cavitation and Dynamic Problems in Hydraulic Machinery and Systems, Oct 2007, Timisoara, Romania. hal-00266170

HAL Id: hal-00266170

<https://hal.science/hal-00266170>

Submitted on 14 Jan 2020

HAL is a multi-disciplinary open access archive for the deposit and dissemination of scientific research documents, whether they are published or not. The documents may come from teaching and research institutions in France or abroad, or from public or private research centers.

L'archive ouverte pluridisciplinaire **HAL**, est destinée au dépôt et à la diffusion de documents scientifiques de niveau recherche, publiés ou non, émanant des établissements d'enseignement et de recherche français ou étrangers, des laboratoires publics ou privés.



Distributed under a Creative Commons Attribution 4.0 International License

A INNOVATIVE MODELLING APPROACH TO INVESTIGATE THE EFFICIENCY OF CROSS FLOW WATER TURBINE FARMS

Sylvain ANTHEAUME *

Laboratoire des Ecoulements Géophysiques et industriels,
Electricité De France

Thierry MAÎTRE

Laboratoire des Ecoulements Géophysiques et industriels,
Institut National Polytechnique de Grenoble

Jean-Luc ACHARD

Laboratoire des Ecoulements Géophysiques et industriels,
Institut National Polytechnique de Grenoble

**Corresponding author:* LEGI, 1023 rue de la Piscine, BP 53, Saint-Martin-d'Hères Cedex 9 - France
Tel.: +33476825116, E-mail: Sylvain.Antheaume@hmg.inpg.fr

ABSTRACT

In 2001, the Geophysical and Industrial Fluid Flows laboratory (LEGI-France) launched the HARVEST research program (**H**ydroliennes à **A**xes de **R**otation **V**ertical **S**tabilisé) to better understand and develop a suitable technology for hydroelectric marine or river power farms using **C**ross **F**low **W**ater **T**urbines (CFWT) piled up in towers. The LEGI researches deal with the hydrodynamic part of these systems, with the support of the R&D Division of the EDF Group; other laboratories of the Rhône-Alpes Region are in charge of the respective mechanical (3S-INPG and LDMS-INSA) and electrical aspects (LEG-INPG).

The present study deals with the study of CFWT arrangements. In a first part, a single turbine for free fluid flow conditions is considered. The simulations are carried out with a new in house code which couples a Navier-Stokes computation of the outer flow field with a description of the inner flow field around the turbine. The latter approach is validated with experimental results of a Darrieus wind turbine in an unbounded domain. This code is then applied for the description of a hydraulic turbine. We then pile up these turbines in the shape of towers and study the efficiency of several lined up towers which makes a barge. Simulations are now bidimensional and show that the average barge efficiency rises as the distance between towers is decreased. Eventually an HARVEST farm, consisting of several barges is investigated. Aligned and staggered rows architectures are considered. Results show that staggered rows architecture is more interesting provided enough space is let between rows.

KEYWORDS

Cross flow water turbine, farm modelling, efficiency

INTRODUCTION

Exhaustion of fossil fuels resources combined with greenhouse gas negative impact have recently raised the interest for renewable energies. Among them; hydropower takes a particular place because of its huge potential. Large-hydro power plants are being built in countries such as Brazil, China or Turkey that exploit a minor part of their hydroelectric potential. Concerning countries historically well equipped, located in Europe and North America, ambitious upgrading programs are carried out to raise the extracted power of existing plants. Numerous Micro-hydro power plants, presently build on rivers and canals, contribute also to the global growth of the hydropower production.

Beyond this classical hydroelectricity, the exploitation of the ocean tidal energy is particularly attractive because it represents a huge and practically inexhaustible source of energy easily accessible on coastal sites. Though the “La Rance” tidal power plant build in 1967 in France is a technological success, it seems that harnessing the energy of the tidal currents, rather than the tidal head as done in La Rance, could be an interesting alternative. The reason is that harnessing currents do not need a dam along the coast and consequently remove the problem of its negative environmental impact. The exploitable part of the tidal kinetic energy over the European shore is estimated to 48 TWh, a significant potential contribution in

comparison with the European hydroelectric production of 580 TWh.

By installing marine current energy converters (turbines), in tidal currents, some of their kinetic energy can be recovered. The English and Norwegians have already installed prototypes of axial flow (horizontal-axis) marine current energy converters. The 1.2 MW bi-rotor English prototype Seagen is planned to be installed in 2007.

Although the axial flow marine current energy converter design is an attractive idea, as it is based on proven technology, it is not the design chosen by the LEGI laboratory. This laboratory, within the HARVEST project [1], develops its own concept based on cross flow current energy converters (vertical axis, or Darrieus, turbines). The main advantage of these converters is their ability to operate irrespective of the direction of the current. The vertical axis also allows the marine current energy converters to be stacked on a single rotation axis called a "turbine axis" that is held firmly in place by a lattice structure called a "tower" (Fig. 1) [2]. The towers are assembled in groups to form a barge anchored to the sea bed. Several barges make a farm. These devices could also be well adapted to extract kinetic energy in rivers. In this case, towers could be anchored separately.

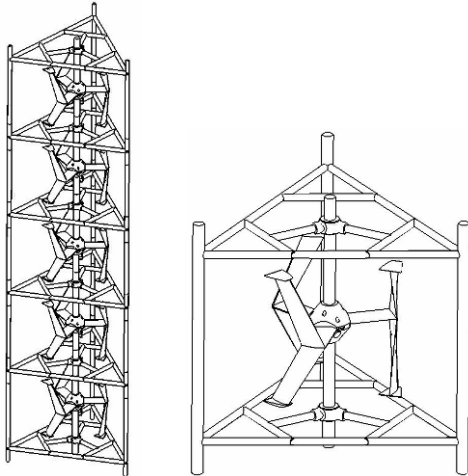


Figure 1. Achard turbine and tower

Concerning the turbine, it is possible to shape blades in such a way that cyclic loading induced by cross flow turbines in air are strongly decreased in water. Consequently, fatigue phenomena are reduced and the life time of the converter is increased. To fulfill this need, Alexandre Gorlov proposed an helical blade shape turbine [3]. The present LEGI-Achard turbine uses delta blades (Fig. 1) [4].

One of the major objectives of the HARVEST project is that it will gradually lead to the construction of marine and river cross flow hydropower farms incorporating the technical solutions defined by the researches undertaken by the four laborato-

ries of the French Rhône-Alpes Region: LEGI, 3S, LDMS, LEG. The HARVEST project is supported by an experimental program dealing with rivers applications in a first step and with ocean applications in a second step.

Modeling tools are developed for hydrodynamic, electric or mechanical issues. The present study concerns the study of the efficiency of towers and barges configurations. Computations are made with a in-house code that couple a macroscopic model of the tower [5] with a RANS calculation of the flow field [6].

1. METHOD OF SOLUTION

In order to design MCEC farms, it is necessary to develop a numerical model for cross flow turbines. This model has to be accurate enough to predict the main performance characteristics of an isolated turbine: power, drag, wake...but it also needs to be fast and thus quite simple to be able to be used for the simulation of farms of many MCEC.

There are existing simplified models which use macroscopic mass and momentum balances to predict the performance of cross flow turbine, in function of the tip speed ratio of the blades $\lambda = \omega R / V_0$ [7,8]. However, they are limited to turbines which solidity doesn't exceed 0.25, corresponding to air flow applications and are then inappropriate for the simulation of future MCEC ($0.5 < S < 1$ for water applications) [7,9,10]. That's why a new CFD-macroscopic coupled code has been developed.

The macroscopic flow field is solved with the commercial code *Fluent* using a k- ϵ turbulence model and a steady state formulation. The turbine perturbation of the incoming free flow is modelled, within the turbine swept volume, with a volume force introduced in the right hand side of the momentum equation. This source term corresponds to the aforementioned inner or microscopic part of the solution. It can be obtained in two ways, either from experimental data or by solving the inner problem which corresponds to computing the solution around an airfoil in an unbounded domain.

In the present method, the blade source terms are evaluated using the Blade Element Theory, requiring the aerodynamic coefficients of the blades. For a straight Darrieus turbine, the swept volume is an annular cylinder of blade thickness, centred on the turbine axis of rotation. It is meshed with N_{cell} structured annular cells of $\Delta\theta$ angular size and ΔZ axial size (Fig. 2). The mesh is uniform along the θ direction and is refined in the Z direction at the tip of the turbine.

Let's consider a cell in the swept volume and suppose that a guess of the flow field is known (for example an arbitrary initialization of the flow needed by a RANS solver). Then it is possible to compute,

at the centre of the cell, the local relative velocity W and the local angle of attack α between W and the chord. The instantaneous lift and drag force applied on the part ΔZ of the blade span centred on the considered cell is given by:

$$F_{L,D} = C_{L,D}(\alpha, Re_C) C \Delta z \frac{1}{2} \rho W^2 \quad (1)$$

where C_L and C_D are respectively the static lift and drag coefficients of the blade section and $Re_C = R\omega C/\nu$ is the chord Reynolds number

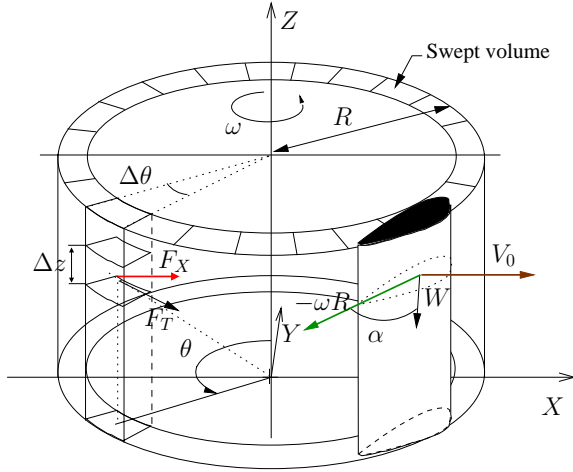


Figure 2. Schematic view of the discretized swept volume

The force applied on the flow by the blade element can be easily expressed in the fixed system coordinate (O,X,Y) by projection of F_L and F_D on the X and Y axis (the minus sign coming from the action/reaction principle). The obtained components, F_X and F_Y , cannot be directly introduced as source terms because they are instantaneous and consequently not consistent with the expected steady state solution. Actually, the correct terms correspond to the mean time value of F_X and F_Y on a period of revolution. Assuming a constant rotational speed of the turbine and considering that the hydrodynamic forces are:

- constant when the quarter chord blade point is in the cell;
- 0 when it is out.

the time averaging operation leads simply to a multiplicative factor $N\Delta\theta/2\pi$ for a N bladed turbine. As a result, the corresponding average values F_{Xcell} and F_{Ycell} of F_X and F_Y are the following:

$$F_{X,Ycell} = F_{X,Y} N\Delta\theta / 2\pi \quad (2)$$

For each cell lying in the swept area, F_{Xcell} and F_{Ycell} are divided by the cell volume before being introduced in the X and Y momentum equations. This operation is done at every iteration of the solver until the turbine efficiency (or drag) stabilized. Every iteration, several coefficients of interest are calculated.

The turbine drag coefficient:

$$C_D = \frac{\sum_{i=1}^{N_{cell}} F_{Xcell}}{1/2\rho S_{ref} V_0^2} \quad (3)$$

the turbine lift coefficient:

$$C_L = \frac{\sum_{i=1}^{N_{cell}} F_{Ycell}}{1/2\rho S_{ref} V_0^2} \quad (4)$$

the turbine power coefficient:

$$C_P = \frac{\sum_{i=1}^{N_{cell}} R F_{tcell}}{1/2\rho S_{ref} V_0^3} \quad (5)$$

where F_{tcell} is equivalent of F_{Xcell} and F_{Ycell} for the tangential component

The following sections present results obtained with the *Fluent* solver. The above calculations are performed using the User Defined Functions.

In all the test cases, the *Fluent* solver parameters are listed below:

- segregated solver;
- pressure-velocity coupling: simple;
- standard discretization for pressure; first order upwind for momentum, turbulence kinetic energy, turbulence dissipation rate;
- standard k-ε turbulence model.

The boundary conditions used for the domain are:

- velocity inlet condition at the upstream boundary;
- pressure outlet condition for the downstream boundary;
- walls with zero shear stress for others domain frontiers;
- symmetry condition at the meridian plane to minimize computational effort when running 3D simulations.

Figure 3 shows an upper view of the straight Darrieus turbine grid, in the X-Y plane (valid in 2D and 3D) and Fig. 4 presents a zoom of the turbine area. The grid density depends directly of the size $\Delta\theta$ of the cells describing the annular swept area (in dark on Fig. 4).

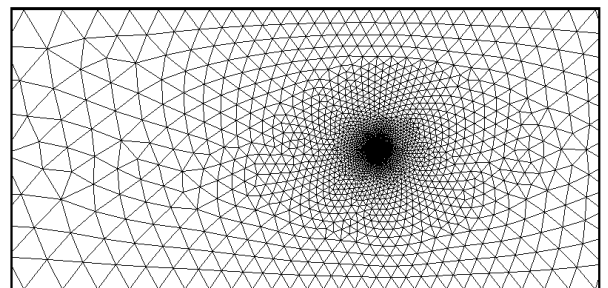


Figure 3. 2D grid up view

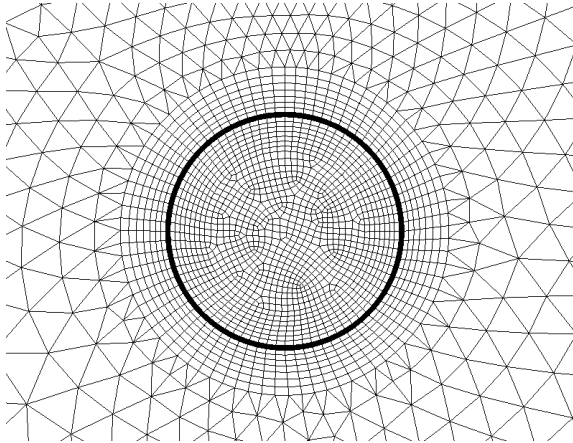


Figure 4. Zoom of the turbine area

2. SINGLE CFWT : EVALUATION OF THE CODE, COMPARISON WITH EXPERIMENT

2.1. The Sandia wind turbine experiment

Darrius turbines were initially developed for wind power generation. The SANDIA laboratories run intensive experiments for many wind turbine configurations and blade profiles and provide a rich data-base of experimental results.

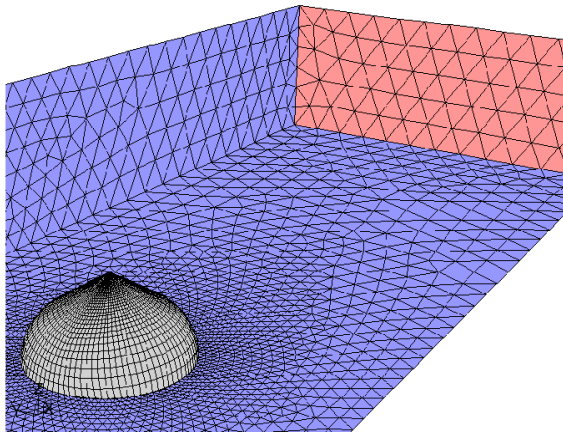


Figure 5. Mesh of the SANDIA experiment

To evaluate the present method, 3 blade configurations of a 2 m diameter Darrius wind turbine with NACA-0012 airfoils are chosen [11]. The geometrical difference between the 3 configurations is the solidity of the turbines. A summary of the experimental test conditions is given in Table 1. Measurements have been carried out in the *Vought Corporation Low Speed Wind Tunnel* (Fig. 6).

For each configuration, the turbines were operated at constant rotational speed. The wind velocity was adjusted to obtain the desired value of tip speed ratio. The steady-state turbine torque was measured to determine the power coefficient. Because the chord Reynolds number Re_C doesn't change within the whole range of tested tip speed ratio λ , only one data set of hydrodynamic coefficients C_L, C_D for a given Re_C of about 150000 is used to run the simulations.

Table 1. Experimental test configurations

Config number	Number of blades	Solidity (%)	Rotor Speed (rpm)	Chord (cm)	Chord Reynolds number
1	3	24.45	267	8.815	150000
2	3	22	320	7.346	151000
3	3	17.63	400	5.877	154000

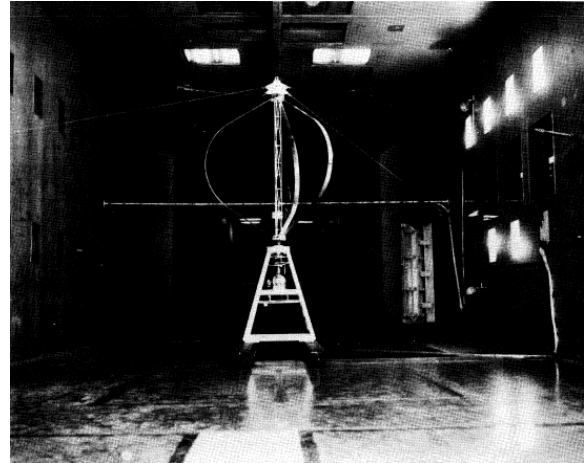


Figure 6. Vought Corporation Low Speed Wind Tunnel

Calculations are run in water using the geometrical dimensions of the wind tunnel and of the turbine. To fulfill the similarity conditions, the chord Reynolds number Re_C and the tip speed ratio λ are kept equal. These conditions give the rotational velocity and the upstream velocity for the simulation.

The NACA-0012 hydrodynamic coefficients are obtained from SANDIA experimental data [12]. The zero drag coefficient C_{D0} corresponding to a 0 angle of attack is corrected to take into account the additional drag due to other rotating parts of the turbine. This additional drag is obtained by spinning the rotor in still air. The same method is used in [7].

Figure 7 shows a good agreement between experimental and calculated power coefficients, especially in the ranges of λ above the value corresponding to the maximum C_p . In these regions the flow is dominated by the so called "secondary effects" corresponding to a viscous attached flow. The good quality of the comparison is mainly due to adjusting the C_{D0} value. In the range of λ below the maximum C_p , a significant difference is observed between calculated and experimental C_p . This gap is mainly due to the dynamic stall phenomenon (called "primary effects") that a rotating blade exhibits. The associated complex interactions between blades and shed vortices lead to strong unsteady effects revealed by a hysteresis loop for the blade loading [13]. Though the dynamic stall phenomenon can be taken into account by some semi empirical corrections [14] it has not been done in this study for two reasons.

First of all, the influence of these corrections on the mean power and drag coefficients are of second

order for nominal tip speed ratios which corresponds to moderately stalled regime.

Secondly, they are not directly linked with the objective of the present study which focuses on the limitation of the by-pass effect around a CFWT when inserted in a cluster of columns.

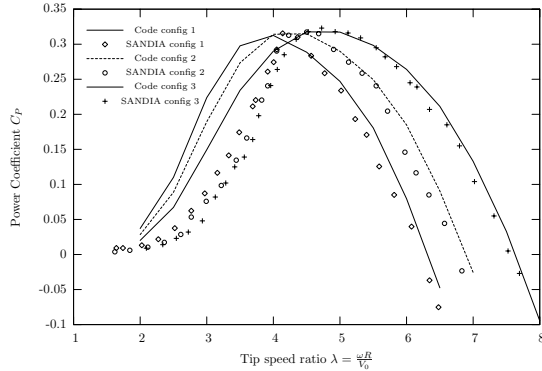


Figure 7. Comparison between SANDIA experiment and code, $Re_c = 150000$

2.2. Straight Darrieus Hydraulic Turbine for free stream conditions

The present numerical model has been tested in the cases of three parabolic Darrieus wind turbines. For large dimensions, these turbines can reach an efficiency up to 0.45, a little bit less than modern axial flow turbines. These performances are obtained with moderate solidity $[0.15-0.25]$ for a tip speed ratio about 5 to 6.

As mentioned above, the future power farm studied in the HARVEST project is based on turbines equipped with delta wings. These turbines are expected to be more efficient than classical straight blade Darrieus turbine (23%) [15] thanks to a reduction of the tip vortex induced drag. Other water turbines have already attained a better efficiency. For example Gorlov obtained 35% with its helical turbine in the Cap Cod Canal [9] and a similar turbine tested in the open jet tunnel of TU Delft exhibited 0.29% [16] confirming the interest of the helical shape. Faure [17] obtained good efficiencies on straight blade Darrieus turbines (more than 40%) but the experiments were purely 2D, leading probably to a smaller influence of tip vortices. Generally, it is observed that an increase of performance produces an increase of tip speed ratio at maximum efficiency leading the designer to shape turbines with smaller solidity.

For the next simulations purpose, a typical HARVEST CFWT is chosen. The diameter and height are both set to 1m, the solidity is set to 0.6 and the upstream velocity V_0 is set to 3 m/s. The diameter based Reynolds number $Re_D = V_0 D / \nu$ is equal to $3 \cdot 10^6$. The maximum efficiency of this turbine, operating alone at free fluid flow conditions, is set to 29%, corresponding to an average between the worst

(23%) and the best (35%) efficiency of similar CFWT. Notice that this choice is not so important, arguing the fact that the aforementioned involved issues do not depend (at least qualitatively) of the exact performance of the turbine. Calculations are performed with the 3D code using the same data set as in Sec. 2.1 The only difference concerns the zero drag coefficient C_{D0} adjusted to fit the required 29% maximum efficiency.

To compare the efficiency of the isolated turbine with a purely 2D isolated tower based on the same turbine, 2D calculations are also performed. In this case, two higher solidities 0.8 and 1 have been also considered. Figure 8 presents the power coefficient against the tip speed ratio for the three 2D isolated towers and for the 3D isolated turbine. One can observe first that the code is able to simulate high solidities contrary to the existing global models [7]. Then, it accurately represents the effect of changing blade solidity (i.e with increased solidity, the maximum power coefficient and the optimal tip speed ratio decreases). Finally, results show that the maximum efficiency of the purely 2D isolated CFWT tower is 34.85%, 5.85% more than the 3D isolated CFWT.

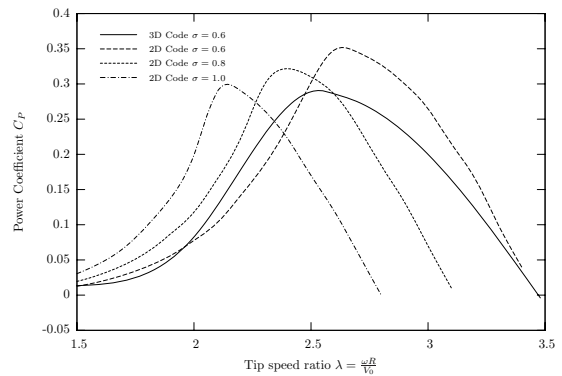


Figure 8. Power coefficient for three 2D and one 3D hydraulic turbines simulations, $Re_D = 3 \cdot 10^6$

3. THE BARGE CONFIGURATION

The towers can be aligned within a cluster which represents a potential barge. The objective of this section is to investigate the influence of the tower spacing on the average efficiency of a cluster (ie the mean efficiency of the towers). To simplify the analysis, purely 2D towers of Sec. 2.2 are considered. The chosen solidity is 0.6 and all CFWT operate at the same rotational speed corresponding to the optimal $\lambda = 2.65$ for an isolated configuration. The corresponding maximum efficiency is 34.85% (Fig. 8).

The test consists in moving closer 5 towers to investigate the effect of tower spacing on the maximum average efficiency. One can notice on Fig. 9 that the closer the barges, the better the efficiency. Once again, this result can be explained by the velocity streamlines straightening effect of the configuration (Fig. 10).

For a lateral spacing of 1.5 turbine diameter, the maximum average efficiency reaches 39.32%, 4.5% more than for the single isolated tower. However, we have to be cautious regarding the feasibility of such a close up barge. For instance, we can expect that it would be prohibited to prevent the towers from knocking with each other or to let enough space for the aquatic fauna.

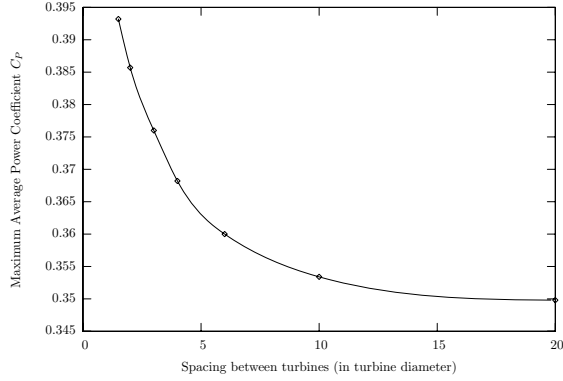


Figure 9. Spacing turbine effect on performance

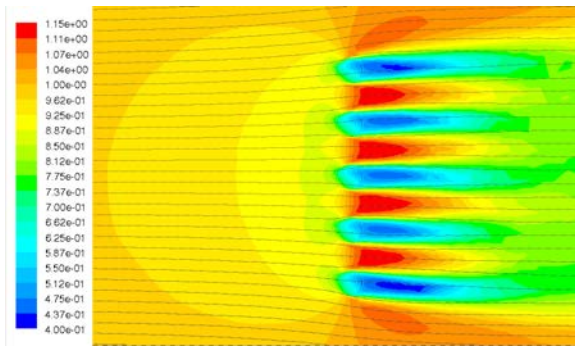


Figure 10. Velocity streamlines in the barge region colored with the reduced velocity V_x/V_0 , 2 turbines diameter spacing between turbines

4. FARM MODELLING

In this section, we deal with the optimization of cross flow water turbine farms. The barges are made of 6 towers of 3m diameter and 0.6 solidity and the upstream velocity is kept equal to 1m/s leading to the same Reynolds number as in the above section $Re_D = 0.3 \cdot 10^6$. The farms are composed of 32 barges arranged in 4 rows of 8 barges. For the barge, a spacing of $3.13 D_t$ is taken considering that a smaller value could be problematic for a realistic exploitation. Doing so, the width of the barge is equal to 50 m.

Since, there are 192 turbines to model, the mesh is simplified to minimize the computational effort. Therefore, in this simulation, the turbines are square shaped and represented with four rectangular cells. Due to this simplification, the procedure for calculating source terms (see Sec. 1) is slightly modified. An average turbine velocity is calculated using the centred values of the four cells. This unique velocity is used to compute the local relative velocity W at

blade location whatever its position θ on the circle of rotation. Then $F_{X_{cell}}$ and $F_{Y_{cell}}$ are calculated using Eq. 2 with a small enough $\Delta\theta$ (that do not correspond to any mesh in the swept region). The total drag F_D and lift F_L applied on the flow by the turbine is obtained using Eq. 3. F_D and F_L are divided by the surface of the four cells, simulating the turbine, and are respectively introduced as source terms in the x and y momentums equations of the solver. This new simplified procedure modifies somewhat the results of the “original code”. The “farm code” leads to higher C_p values at high tip speed ratios. However, though a new source of uncertainty appears with the use of the farm code, it allows to highlight some tendencies for the efficiency when varying parameters describing the farm architecture.

Simulations of farms are carried out for a single value of the tip speed ratio $\lambda = 2.65$ corresponding to the maximum C_p for the 0.6 solidity 2D single turbine (see Fig. 8).

The aligned row configuration (ARC) and staggered rows configuration (SRC) are going to be tested (Fig.11). IN each case, we investigate the influence of lateral L and longitudinal spacing l over the performance of the farm, in a way similar to the study performed by EDF R&D [21]. In the following section D_b represents the width of a barge.

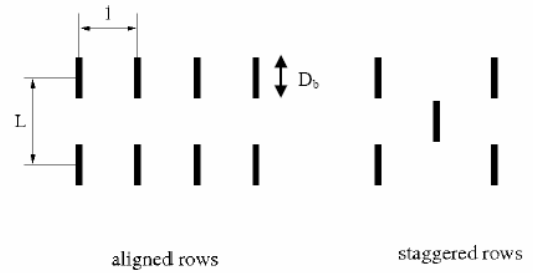


Figure 11. Tested farms architectures

4.1. Aligned rows

The table 2 presents the loss of power of the simulated farm compared with a reference farm¹ made of 192 independent turbines. The first conclusion is that the closer the barges, the greater the loss. Indeed, the downstream rows of barges are in the wake of the upstream rows, resulting in a loss of incoming kinetic energy and thus responsible for the loss of power. For example, we have 35% of loss in the $10D_b/2D_b$ ARC configuration. IN this case, the first row runs at 100% of its maximum, then 74%, 52% and 39% respectively for the second, third and fourth rows. For the ARC $30D_b/8D_b$ case, there is only 8.6% of loss. This corresponds to power ratios of 100%, 93%, 89% and 84% respectively for rows 1,2,3 and 4. The

¹ The definition of the reference farm is not unique. It could be a farm made of 32 independent barges. This would lead to higher values of loss in Tab. 2 and Tab. 4

fluid retrieves most of its kinetic energy between rows. However, we have to keep in mind that one of the main constraint about the marine farms is the total surface taken up over the sea. Thus, it is interesting to look at another variable which is the average power delivered per unit surface, in kW/m². The table 3 shows that, even if the small surfaces configurations have the highest losses, they have the most interesting ratios of power per unit surface.

Table 2. Loss of power relatively to the reference farm [%], ARC, $E = 3.13Dt$

l/L	2D _b	4D _b	6D _b	8D _b
10D _b	35	30.6	30.4	29.5
20D _b	31.3	18.5	14.8	14.1
30D _b	28.9	16.1	10.4	8.6

Table 3. Power per unit surface [kW/ m²], ARC, $E = 3.13Dt$

l/L	2D _b	4D _b	6D _b	8D _b
10D _b	77	43	29	22
20D _b	41	25	18	13
30D _b	29	17	12	10

4.2. Staggered rows

To minimize the loss of power of the rear lines, a possible idea is to move 1 line out of 2 so that the barges are not in the wake of the barges just in front of them. We will call this barges distribution the staggered row configuration (SRC).

Table 4 shows that the SRC becomes very interesting if the lateral spacing is equal or greater than 4D_b. For example, the 10D_b/4D_b SRC loss is 9.7% whereas the 10D_b/4D_b ARC loss is 30.6%. A great decrease of loss is also obtained with the SRC the 10D_b/6D_b and 20D_b/6D_b configuration in comparison with the same ARC configurations. It is also observed that the SRC 20D_b/4D_b configuration is worst than the 10D_b/4D_b (16.7% against 18.5%). For lateral spacing $L = 2D_b$, the SRC configurations lead also to an increase of loss when the longitudinal spacing l is increased. These particular wake effect occurs in the SRC configurations when downstream barges are too far of upstream one comparatively to their lateral distance. Concerning the power per unit surface (Tab. 5), the same conclusion as for ARC configurations is obtained: the best ratio corresponds to the smallest farm (5D_b/2D_b).

Table 4: Loss of power relatively to the reference farm [%], SRC, $E = 3.13Dt$

l/L	2D _b	4D _b	6D _b
5D _b	28.6	8.9	8.6
10D _b	31.3	9.7	5
20D _b	31.8	16.7	7.6

Table 5: Power per unit surface [kW/ m²], SRC, $E = 3.13Dt$

l/L	2D _b	4D _b	6D _b
5D _b	170.5	112.5	76.15
10D _b	82	55.8	39.6
20D _b	40.7	25.7	19.3

However, even if a high power density farm is found, it might be banned since it creates a high global drag and a high reduction of the flow passage. The price per unit power also has to be taken into account and might be excessively high for these configurations. That's why, a wise choice for a future farm could be for SRC architectures of more than 4D_b of lateral spacing. In this case, the SRC sounds to be a good candidate compared to the ARC, especially for medium size farms. Indeed, we can take for example the SRC 10D_b/6D_b configuration which registers a loss of 5% instead of 30.4% in the ARC case. As the size of both farms is the same, power per unit surface is also better for the SRC configuration: 39.6 kW/ m² against 29 kW/ m² for ARC. Eventually, we have to remember that all the power values given in this section correspond to an upstream velocity of 1m/s. Neglecting the Reynolds number effect, these values increase with the cubic power of the upstream velocity.

CONCLUSION

A powerful and reliable modelling too, especially well adapted for the simulation of cross flow water turbines has been developed. The code has been evaluated on a single machine by comparison with the SANDIA experiment. The 2D code version has then been used for the optimization of a barge made of lined columns of CFWT. Results show that an increase of efficiency as the towers are settled closer. We observe a maximum average efficiency of 39.4% for a lateral spacing of 1.5 Dt. This is 4.55% more than for a single 2D isolated tower and 10.4% more than for the 3D reference hydraulic turbine. In the meantime, the final configuration of a barge is not definitive because there is a lack of knowledge about the minimal distance to keep between units. There also might be many others barges architectures. A set of simulations on different farms configurations have raised the conclusion that the large farms loose less energy than the closed up ones but have worse ratios of power per unit surface. We also have demonstrated the interest of the staggered rows configuration to limit the wake effect.

ACKNOWLEDGEMENTS

Authors gratefully acknowledge the R&D Division of the EDF Group for its technical and financial support.

NOMENCLATURE

C	= blade chord
C_p	= power coefficient of the turbine
C_D	= drag coefficient of the turbine
C_{D0}	= zero lift drag coefficient
C_n	= normal force coefficient
C_t	= tangential force coefficient
D	= turbine diameter
D_b	= barge width
D_t	= spacing between turbines within a barge
F_D	= drag force applied on the flow by the turbine
F_L	= lift force applied on the flow by the turbine
F_n	= radial force on a blade
F_t	= working force on a blade
F_{tcell}	= tangential force applied on the flow by a cell
F_{Xcell}	= drag force applied on the flow by a cell
F_{Ycell}	= lift force applied on the flow by a cell
L	= lateral spacing between barges
L	= longitudinal spacing between barges
H	= turbine height
N	= number of blades
N_{cell}	= number of cells in the turbine swept volume
n	= radial direction
Q	= turbine torque
R	= turbine radius
Re_C	= $R\omega C/\nu$, chord based Reynolds number
Re_D	= $V_0 D/\nu$, diameter based Reynolds number
S_{ref}	= DH , turbine reference surface
t	= tangential direction
V_0	= upstream velocity
W	= relative velocity
$O X Y$	= cartesian coordinate system
α	= blade incidence angle
λ	= $R\omega/V_0$, tip speed ratio
ω	= rotational velocity
θ	= rotational angle
$\Delta\theta$	= cell angular size
σ	= NC/R , solidity

REFERENCES

- [1] Maitre, T., and Achard, J-L., Mai 2003, « Une source d'énergie renouvelable possible: les Hydrauliques », *Revue de l'Energie*, **546**, pp. 315–319.
- [2] Achard, J-L., and Imbault, D. and Maitre, T., 14 Février 2005, « Dispositif de maintien d'une turbomachine hydraulique », Brevet déposé : Code : FR 05 50420, Titulaires : INPG.
- [3] Gorlov, A.M., 1st July 1997, "The Helical turbine assembly operable under multidirectional fluid flow for power and propulsion systems". United States Patent N°5,642,984.
- [4] Achard, J-L., and Maitre, T., 4 Février 2004 « Turbomachine hydraulique », Brevet déposé : Code : FR 04 50209, Titulaires : INPG.
- [5] Templin, R., 1974, "Aerodynamics performance theory for the ncr vertical-axis turbine", N.A.E. Report LTR-LA6160.
- [6] Antheaume, S., and Maître, T., and Buvat, C., and Abonnel, C., October 23rd/24rd, 2006, "Optimisation of a vertical axis water turbine power farm", Proc. 1st International Conference Ocean Energy, Bremerhaven, Germany.
- [7] Paraschivoiu, I., 2002, *Wind turbine Design*, Polytechnic International Press.
- [8] Templin, R., 1974, "Aerodynamics performance theory for the ncr vertical-axis wind turbine", N.A.E. Report LTR-LA-160.
- [9] Gorlov, A.M., 1998, "Helical turbines for gulf stream conceptual approach to design of a large-scale floating power farm", *MarineTechnology*, **35**(3), pp. 175-182.
- [10] Takamatsu, Y., and Furukawa, A., and Okuma, K., and Shimogama, Y., 1985, "Study on hydrodynamic performance of Darrieus-type cross-flow turbine", *Bulletin of JSME* **28**(240).
- [11] Sheldhal, R.E., and Blackwell, B.F, 1977, "Free-Air Performances Test of a 5-Meter Diameter Darrieus Turbine", SANDIA Laboratories.
- [12] Sheldhal, R.E., and Klimas, P. C., March 1981 "Aerodynamic characteristics of seven symmetrical airfoil sections through 180-degree angle of attack for use in aerodynamic analysis of vertical axis wind turbines", Tech. Rep. SAND80-2114, SANDIA Laboratories.
- [13] Laneville, A., and Vittecoq, P., 1986, "Dynamic stall: the case of the vertical axis wind turbine", *Journal of Solar Energy Engineering*, **108**, pp. 140–145.
- [14] Fraunié, P., and Beguier, C., and Paraschivoiu, I., 1985, « Importance du décrochage dynamique dans les calculs aérodynamiques du rotor Darrieus », *Journal de Mécanique Théorique et appliquée* **4**(6), pp.785–804.
- [15] Shiono, M., and Suzuki, K., and Kiho, S., 2000, "An experimental study of the characteristics of a Darrieus turbine for tidal power generation", *Electrical Engineering in Japan*, **132**(3), pp. 315–319.
- [16] Van Bussel, G. J. W., 2004, "The development of turby, a small vawt for the built environment", Proc. Global Wind Energy Conference, Delpht, The Netherlands.
- [17] Faure, T.D., and Pratte, B.D., and Swan, D.H., 1986, "The darrieus hydraulic turbine-model and field experiments", Proc. 4th ASME International Symposium for Hydro Power and Fluid Machinery, San Francisco.
- [18] Ponta, F., and Dutt, G. S., 2000, "An improved vertical-axis water-current turbine incorporating a channelling device", *Renewable Energy* **20**, pp. 223–241.
- [19] Blue Energy Canada, 2000, www.bluenergy.com.
- [20] Daviau, J. F., and Majastre, H., and Guena, F., and Ruer, J., 2004, "Divers aspects de l'exploitation de l'énergie des courants marins", Proc. Sea Tech Week, Brest, France.
- [21] Peyrard, C., Buvat, C., Lafon, F., Abonnel, C., October 23rd/24rd, 2006, "Investigations of the wake effects in marine current farms through numerical modeling with the Telemac system", Proc. 1st International Conference Ocean Energy, Bremerhaven, Germany.